

# Quantum design in study of pycnonuclear reactions in compact stars:

*Nuclear fusion, quasibound states, spectroscopy*

**S. P. Maydanyuk**

*(1) Wigner Research Centre for Physics, Budapest*

## **Outline :**

- 1) Potential of nuclear interactions, scattering  $^{12}\text{C}$ - $^{12}\text{C}$  in lattice,
- 2) Method of Multiple Internal Reflections,
- 3) New quasibound states in pycnonuclear reactions,
- 4) Energies of zero-point vibrations of nuclei (Zel'dovich approach).

# Pycnonuclear reactions in compact stars

---

In stars, thermal energy of reacting nuclei overcomes the Coulomb repulsion between them so that a reaction can proceed. At sufficiently high densities, even at zero temperature, energy of nuclei in lattice lead to an appreciable rate of reactions. This phenomenon is known as *pycnonuclear reaction* (from “pyknos” as “dense” in Greek) [1].

Pycnonuclear burning occurs in *dense and cold cores of white dwarfs* [2] and in *crusts of accreting neutron stars* [3].

*Astrophysical S-factors* are estimated for 946 thermonuclear reactions for isotopes C, O, Ne and Mg for energies 2 - 30 MeV [4]. Large database of *S-factors* [5] is formed for isotopes Be, B, C, N, O, F, Ne, Na, Mg, Si (5000 non-resonant thermo-reactions).

[1] A.G.W.Cameron, *Pycnonuclear reactions and nova explosions*, Astr. J. **130**, 916 (1959).

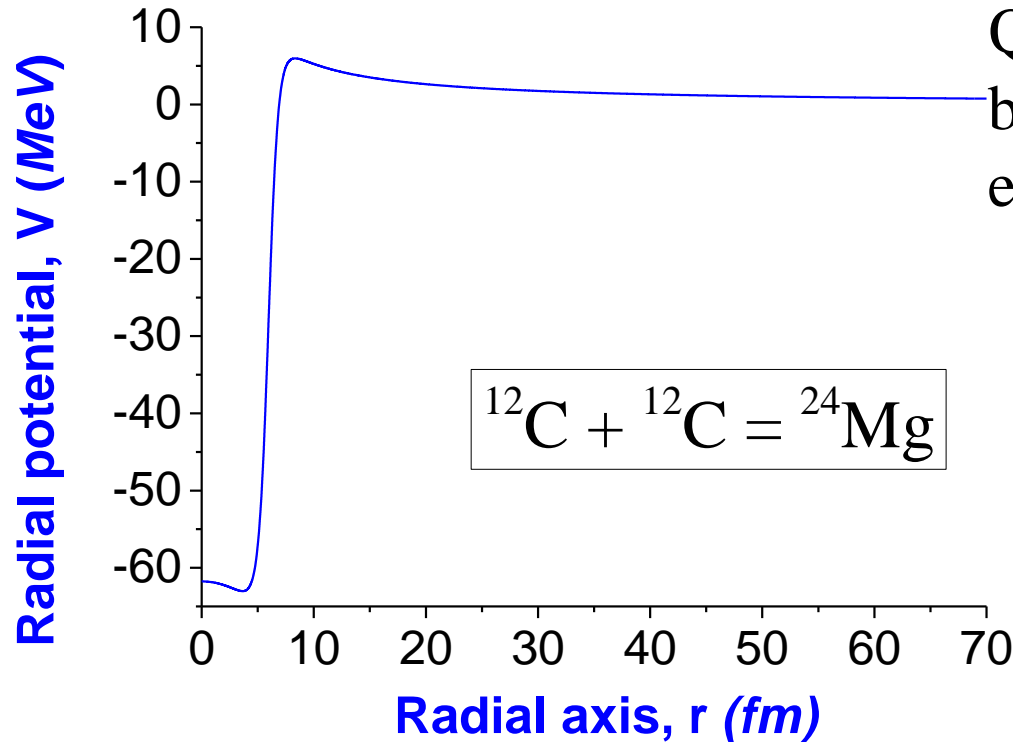
[2] E.E.Salpeter, H.M.VanHorn, Nuclear reaction rates at high densities, Astr. J. **155**, 183 (1969).

[3] P. Haensel/ et al., Astron. Astr. **229**, 117 (1990); **404**, L33 (2003).

[4] M.Beard, A.V.Afanasjev, et al., At. Dat. Nucl. Dat. Tabl. **96**, 541-566 (2010).

[5] A.V.Afanasjev, M.Beard, et al., Phys. Rev. C **85**, 054615 (2012).

# Potential of interactions



Quantum mechanical study on the basis of solution of Schrodinger equation with potential:

$$V(r) = V_C(r) + V_N(r) + V_{l=0}(r),$$

$$V_N(r) = -\frac{V_R}{1 + \exp\left(\frac{r - R_R}{a_R}\right)},$$

$$R_R = r_R (A_1^{1/3} + A_2^{1/3}),$$

$$r_R = 1.30 \text{ fm}, \quad a_R = 0.44 \text{ fm}.$$

$$V = -75 \text{ MeV}.$$

$$\rho_0 = \frac{m_A}{V_A} = \frac{Am_u}{4/3\pi R_0^3},$$

$$R_0 = \left(\frac{Am_u}{4/3\pi \rho_0}\right)^{1/3}. \quad n_A = \frac{\rho_0}{Am_u}.$$

$$\rho_0 = 6 \cdot 10^9 \frac{\text{g}}{\text{cm}^3},$$

$$R_0 = 92.5 \text{ fm},$$

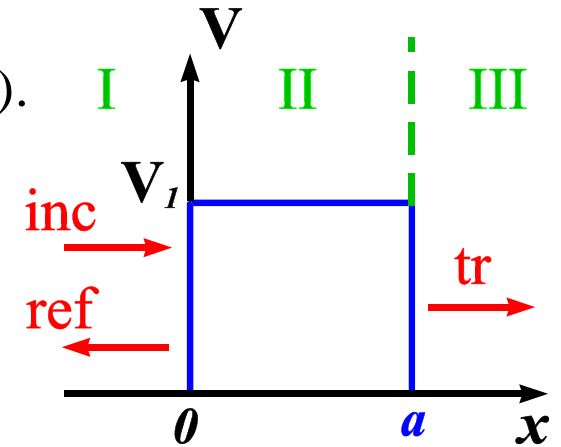
$$n_A = 3.014189 \cdot 10^{-7} \text{ fm}^{-3}.$$

# Method: 1D tunneling (1)

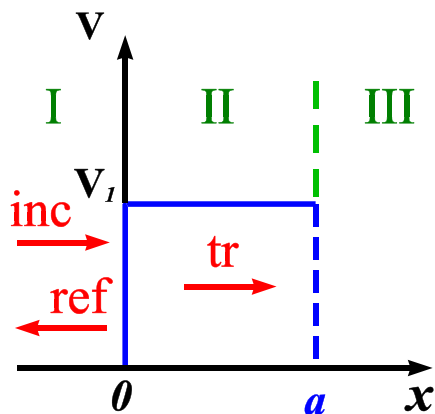
One can understand idea of method the most clearly in the simplest case – analyzing wave, propagating above rectangular barrier.

- Schrodinger equation: 
$$-\frac{\hbar^2}{2m} \frac{d^2}{dx^2} \varphi(x) + V(x)\varphi(x) = E \varphi(x).$$

- Wave function (WF): 
$$\varphi(x) = \begin{cases} e^{ikx} + A_R e^{-ikx}, & x \leq 0, \\ \alpha e^{-ik_2x} + \beta e^{ik_2x}, & 0 \leq x \leq a, \\ A_T e^{ikx}, & x \geq a \end{cases}$$



- Approach on step-by-step:
- Step 1:



$$\varphi_{inc}^{(1)} = e^{ikx}, \quad x \leq 0,$$

$$\varphi_{tr}^{(2)} = \beta^{(0)} e^{ik_2x}, \quad 0 \leq x \leq a,$$

$$\varphi_{ref}^{(1)} = A_R^{(0)} e^{-ikx}, \quad x \leq 0.$$

- Continuity condition at  $x = 0$ :

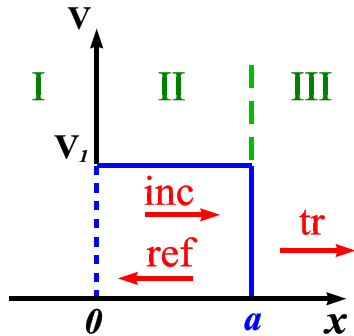
$$\beta^{(0)} = \frac{2k}{k+k_2}, \quad A_R^{(0)} = \frac{k-k_2}{k+k_2}.$$

- Transition to under-barrier tunneling:

$$k_2 \Rightarrow i\xi, \quad k_2 = \frac{1}{\hbar} \sqrt{2m(E-V_1)}$$

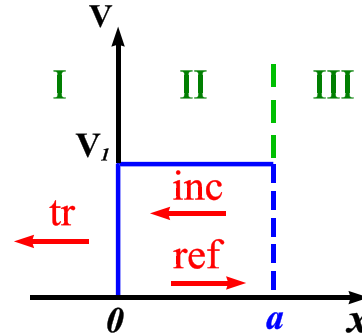
# Method: 1D tunneling (2)

## Step 2:



$$\begin{aligned}\varphi_{inc}^{(2)} &= \varphi_{tr}^{(1)} = \beta^{(0)} e^{ik_2 x}, \\ \varphi_{tr}^{(2)} &= A_T^{(0)} e^{ikx}, \\ \varphi_{ref}^{(2)} &= \alpha^{(0)} e^{-ik_2 x}.\end{aligned}$$

## Step 3:



$$\begin{aligned}\varphi_{inc}^{(3)} &= \varphi_{ref}^{(2)}, \\ \varphi_{tr}^{(3)} &= A_R^{(1)} e^{-ikx}, \\ \varphi_{ref}^{(3)} &= \beta^{(1)} e^{ik_2 x}.\end{aligned}$$

- Continuity WF at  $x = 0, a$ :

$$\alpha^{(n)}, \beta^{(n)}, A_T^{(n)}, A_R^{(n)}$$

- Amplitudes of transmission, reflection:

$$\begin{aligned}A_T &= T_2^+ T_1^- \left( 1 + \sum_{m=1}^{+\infty} (R_2^+ R_1^-)^m \right) = \frac{i4k\xi e^{-\xi a - ika}}{F_{sub}}, \\ A_R &= R_1^+ + T_1^+ R_2^+ T_1^- \left( 1 + \sum_{m=1}^{+\infty} (R_2^+ R_1^-)^m \right) = \frac{k_0^2 D_-}{F_{sub}}\end{aligned}$$

$$F_{sub} = (k^2 - \xi^2)D_- + 2ik\xi D_+, \quad D_{\pm} = 1 \pm e^{-2\xi a}$$

$$k_0^2 = k^2 + \xi^2 = \frac{2mV_1}{\hbar^2}$$

- Coefficients:

$$\begin{aligned}T_1^+ &= \beta^{(0)}, & R_1^+ &= A_R^{(0)}, \\ T_2^+ &= \frac{A_T^{(n)}}{\beta^{(n)}}, & R_2^+ &= \frac{\alpha^{(n)}}{\beta^{(n)}}, \\ T_1^- &= \frac{A_R^{(n+1)}}{\alpha^{(n)}}, & R_1^- &= \frac{\beta^{(n+1)}}{\alpha^{(n)}}\end{aligned}$$

- Test:  $|A_T|^2 + |A_R|^2 = 1$

# Method: Arbitrary number of barriers

Calculation of penetrability for arbitrary number of barriers is essentially more complicated, it has been solved.

- Wave function:

$$\varphi(x) = \begin{cases} e^{ikx} + A_R e^{-ikx}, & x \leq x_1; \\ \alpha_2 e^{ik_2x} + \beta_2 e^{-ik_2x}, & x_1 \leq x \leq x_2; \\ \dots & \dots \\ \alpha_{N-1} e^{ik_{N-1}x} + \beta_{N-1} e^{-ik_{N-1}x}, & x_{N-2} \leq x \leq x_{N-1}; \\ A_T e^{ikx}, & x_{N-1} \leq x \end{cases}$$

- Calculation of coefficients:

$$T_j^+ = \frac{2k_j}{k_j + k_{j+1}} e^{i(k_j - k_{j+1})x_j}, \quad T_j^- = \frac{2k_{j+1}}{k_j + k_{j+1}} e^{i(k_j - k_{j+1})x_j},$$

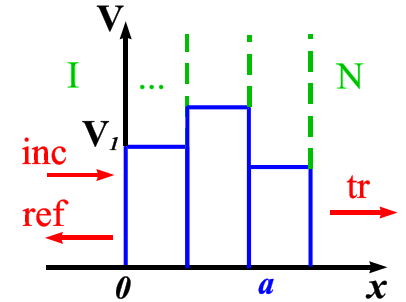
$$R_j^+ = \frac{k_j - k_{j+1}}{k_j + k_{j+1}} e^{2ik_j x_j}, \quad R_j^- = \frac{k_{j+1} - k_j}{k_j + k_{j+1}} e^{-2ik_{j+1} x_j}.$$

- Recurrent relations:

$$\tilde{R}_{j-1}^+ = R_{j-1}^+ + T_{j-1}^+ \tilde{R}_j^+ T_{j-1}^- \left( 1 + \sum_{m=1}^{+\infty} (\tilde{R}_j^+ R_{j-1}^-)^m \right) = R_{j-1}^+ + \frac{T_{j-1}^+ \tilde{R}_j^+ T_{j-1}^-}{1 - \tilde{R}_j^+ R_{j-1}^-},$$

$$\tilde{R}_{j+1}^- = R_{j+1}^- + T_{j+1}^- \tilde{R}_j^- T_{j+1}^+ \left( 1 + \sum_{m=1}^{+\infty} (R_{j+1}^+ \tilde{R}_j^-)^m \right) = R_{j+1}^- + \frac{T_{j+1}^- \tilde{R}_j^- T_{j+1}^+}{1 - \tilde{R}_j^- R_{j+1}^+},$$

$$\tilde{T}_{j+1}^+ = \tilde{T}_j^+ T_{j+1}^+ \left( 1 + \sum_{m=1}^{+\infty} (R_{j+1}^+ \tilde{R}_j^-)^m \right) = \frac{\tilde{T}_j^+ T_{j+1}^+}{1 - \tilde{R}_j^- R_{j+1}^+}.$$



$$\begin{aligned} \tilde{R}_{N-1}^+ &= R_{N-1}^+, \\ \tilde{R}_1^- &= R_1^-, \\ \tilde{T}_1^+ &= T_1^+ \end{aligned}$$

- Amplitudes:  $A_T = \tilde{T}_{N-1}^+, \quad A_R = \tilde{R}_1^+.$

- Penetrability, reflection:

$$T = \frac{k_N}{k_1} |A_T|^2, \quad R = |A_R|^2.$$

# Cross-section of capture

- Cross-section of capture:

$$\sigma_{\text{capture}}(E) = \frac{\pi \hbar^2}{2mE} \sum_{l=0}^{+\infty} (2l+1) T_l P_l.$$

Here,  $E$  is kinetic energy of relative motion of two nuclei in lab. frame,  $E_1$  is kinetic energy of relative motion of two nuclei in the center-of-mass frame (we use  $E = E_1$ ),  $m$  is reduced mass of two nuclei,  $P_l$  is probability of fusion of two nuclei,  $T_l$  is penetrability of barrier.

- Penetrability in WKB-approximation:

$$T_{WKB} = \exp \left\{ -2 \int_{R_{\text{tp},2}}^{R_{\text{tp},3}} \sqrt{\frac{2m}{\hbar^2} (Q_p - V(r))} dr \right\}$$

- Penetrability and reflection for method MR:

$$T_{MIR} = \frac{k_1}{k_N} |A_T|^2, \quad R_{MIR} = |A_R|^2.$$

- Connection with S-factor in astrophysics:

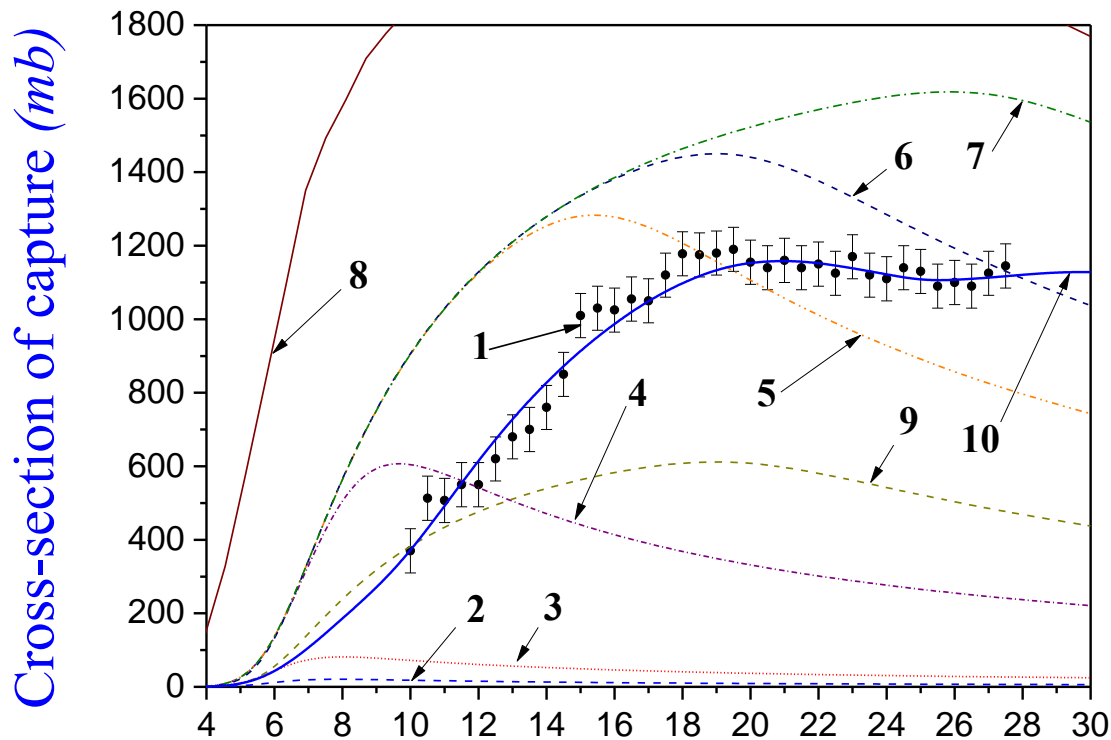
- Test for method MR

- (it is absent in WKB-calc.):

$$T_{MIR} + R_{MIR} + M_{MIR} = 1.$$

$$\sigma(E) = \frac{S(E)}{E} \times T_{\text{full}}.$$

# Cross-section of $\alpha$ -capture: method MIR & WKB



Kinetic energy of  $\alpha$ -particle,  $E_\alpha$  (MeV)

Fig.2. Capture cross-sections of  $\alpha$ -particle by nucleus  $^{44}\text{Ca}$ , obtained by method MIR (lines 2-7, 9-10) and WKB-approach (line 8). Line 10 is obtained at inclusion of probabilities of fusion, lines 2-9 are without fusion prob. [1].

**Conclusion:** Method MIR with included probabilities of fusion (line 10) is in higher agreement with experimental data, than WKB-approach without fusion (line 8).

Black circles 1 is experimental data, dashed blue line 2 is cross-section at  $l_{\max}=0$ , short dashed red line 3 is cross-section at  $l_{\max}=1$ , short dash-dotted purple line 4 is cross-section at  $l_{\max}=5$ , dash-double dotted orange line 5 is cross-section at  $l_{\max}=10$ , dashed dark blue line 6 is cross-section at  $l_{\max}=12$ , dash-dotted green line 7 is cross-section at  $l_{\max}=15$ , solid brown line 8 is cross-section at  $l_{\max}=20$ , dashed dark yellow line 9 is renormalized cross-section at  $l_{\max}=17$ , solid blue line 10 is cross-section at  $l_{\max}=17$ .

■ Cross-section of capture:

$$\sigma_{\text{capture}}(E) = \frac{\pi \hbar^2}{2mE} \sum_{l=0}^{l_{\max}} (2l+1) T_l P_l.$$

Here,  $E$  is kinetic energy of  $\alpha$ -particle in lab. frame,  $E_1$  is kinetic energy of relative motion of  $\alpha$ -particle and nucleus,  $m$  is reduced mass of  $\alpha$ -particle and nucleus,  $P_l$  is probability of fusion of  $\alpha$ -particle and nucleus,  $T_l$  is penetrability of barrier.

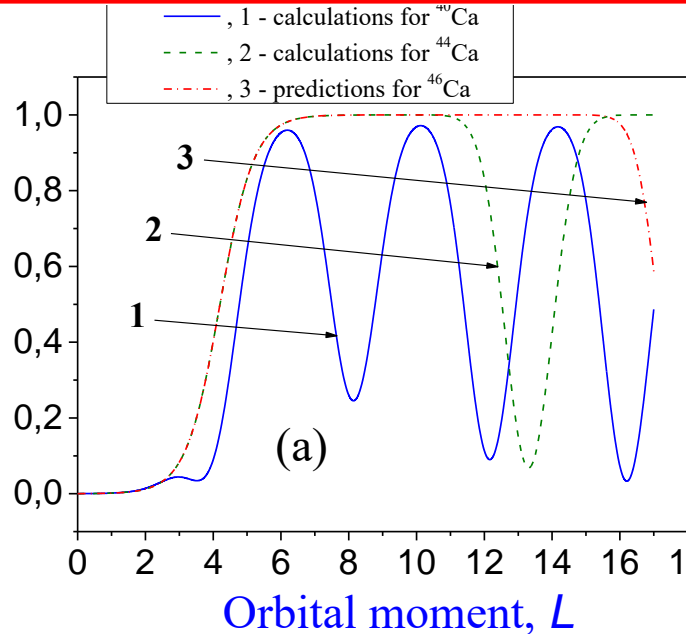
■ Test of method:  $T_{\text{MIR}} + R_{\text{MIR}} = 1$ .

[1] Maydanyuk S. P., Zhang P.-M., et al. Nucl. Phys. **A940**, 89-118 (2015).

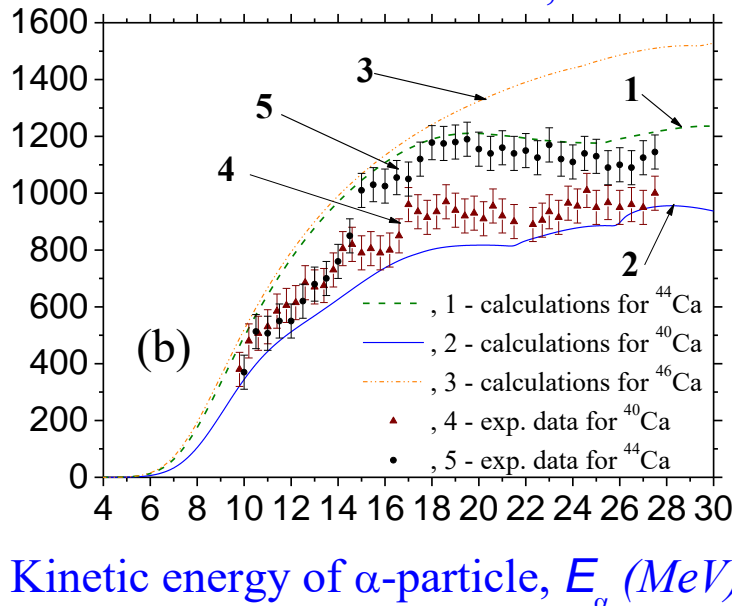


# Formula for probability of fusion

Probability of fusion,  $p_L$



Cross-section of capture (mbarn)



Using fitting procedure, we found probabilities of fusion and described them as

$$\sigma_{\text{capture}}(E) = \frac{\pi \hbar^2}{2mE} \sum_{l=0}^{+\infty} (2l+1) T_l P_l.$$

$$p_{\text{full}}(L) = 1 - p_1(L) - p_2(L),$$

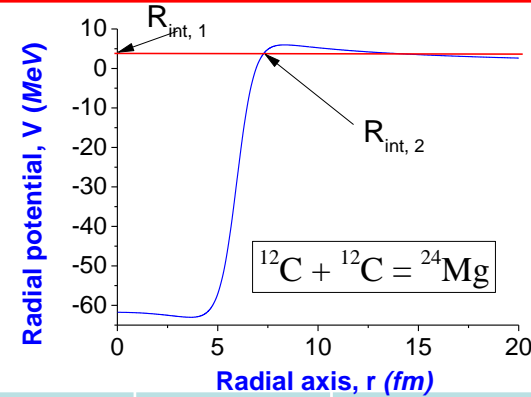
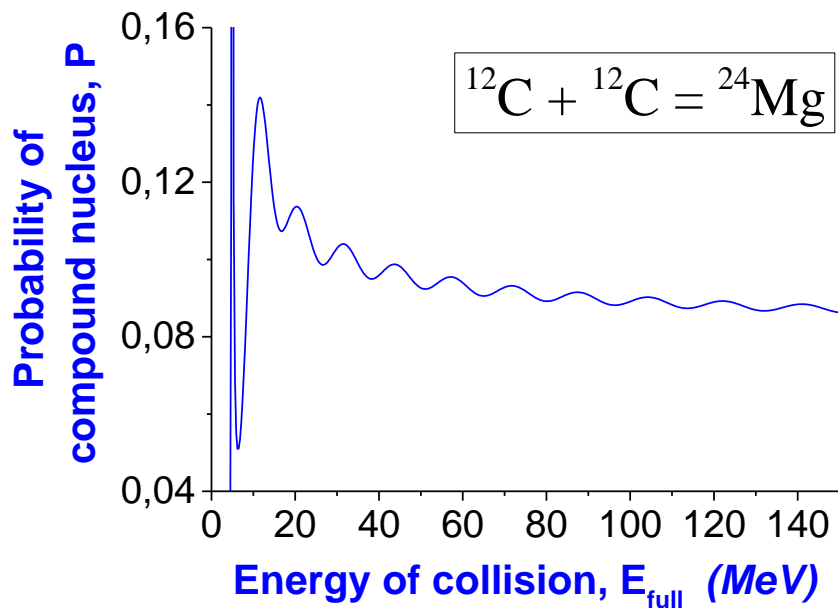
$$p_1(L) = \frac{c_1}{1 + \exp\left[\frac{(L - c_2)}{c_3}\right]}, \quad p_2(L) = f_2(L) \cdot \sum_{n=1} \exp\left\{-\frac{(L - n \cdot \Delta)^2}{c_{4n}}\right\},$$

$$f_2(L) = 1 - \exp\{-c_5 \cdot (L - c_6)\}, \quad \Delta = a \cdot (N - N_{\text{magic}}) + b, \\ a = 2.31, \quad b = 4.05, \quad c_1 = 1, \quad c_2 = 4.2, \quad c_3 = 0.5.$$

Fig.7. Probabilities of fusion (a) calculated by formulas above and cross-sections (b) for capture of  $\alpha$ -particles by  $^{40}\text{Ca}$ ,  $^{44}\text{Ca}$ ,  $^{46}\text{Ca}$ , obtained by method MIR [1].

[1] **Maydanyuk S. P.**, Zhang P.-M., Belchikov S. V. Nucl. Phys. A. - 2015. - Vol. 940. - P. 89-118.

# New quasi-bound states in scattering



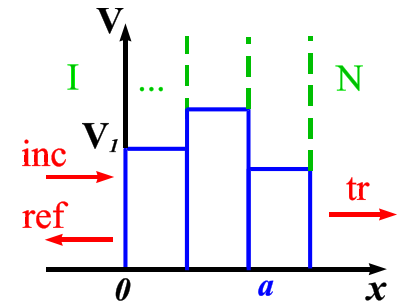
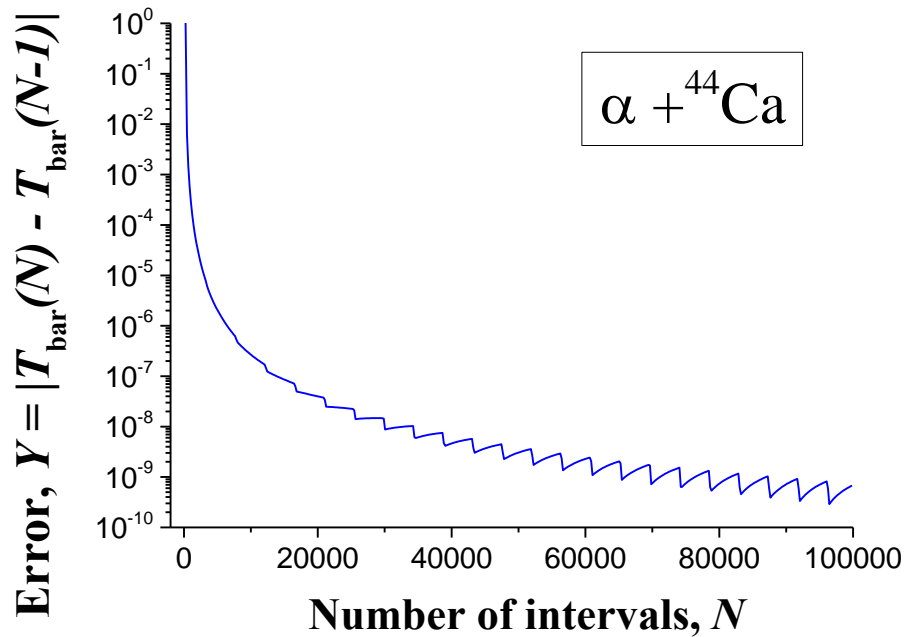
$N$	$E, \text{ MeV}$	$P_{\text{cn}}$	$R_{\text{pot}}$	$R_{\text{res}}$
1	5.0032	0.7805	0.03581	0.6116
2	11.607	0.1419	6.24E-5	0.0038
3	20.313	0.1136	2.07E-6	2.25E-5
4	31.420	0.1040	2.31E-7	1.92E-6
5	43.729	0.0987	4.99E-8	1.71E-8
6	57.238	0.0954	1.57E-8	3.23E-8
7	71.647	0.0931	5.70E-9	3.75E-9

Fig.3. Maximums are clearly visible. These are states of the most probable existence of compound nucleus. We called them as *quasi-bound states in pycnonuclear reactions*.

Probability of existence of compound nucleus:

$$P_{\text{cn}}(E) = \int_{r_{\text{int},1}}^{r_{\text{int},2}} |\chi(r)|^2 dr = \sum_{j=1}^n \left\{ \left( |\alpha_j|^2 + |\beta_j|^2 \right) \Delta r + \frac{\alpha_j \beta_j^*}{2ik_j} e^{2ik_j r} \Big|_{r_{j-1}}^{r_j} + c.c. \right\}$$

# Accuracy of MIR method in capture task

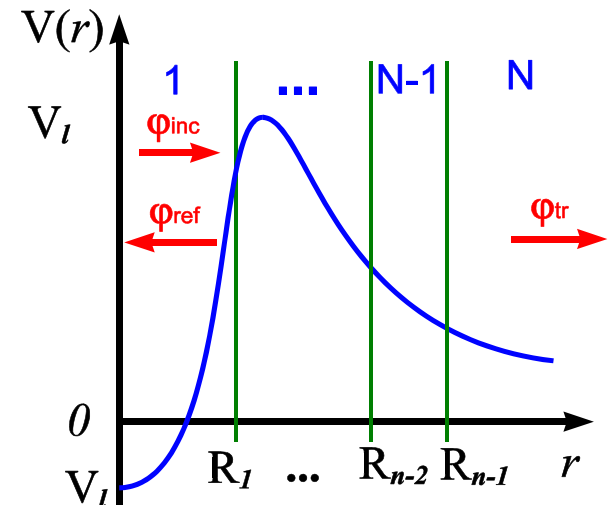


**Test of method:**

$$T_{\text{bar}} + R_{\text{bar}} = 1.$$

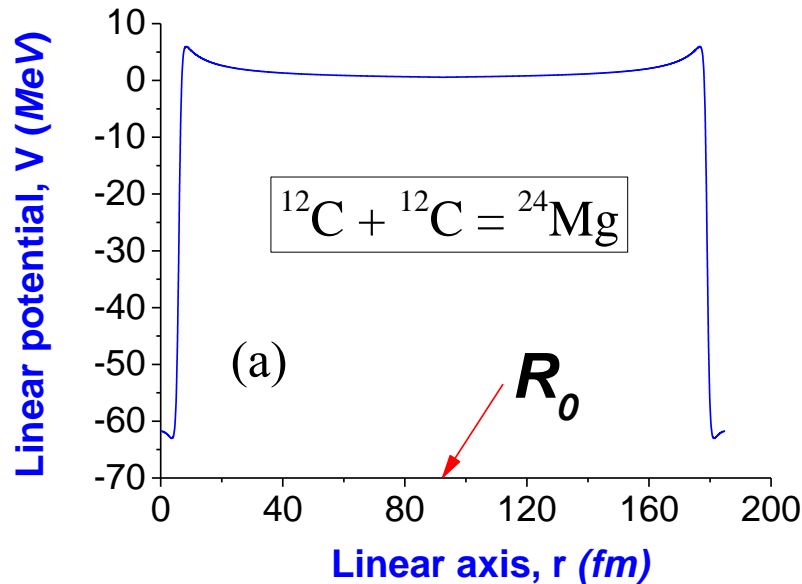
**Accuracy of method:**

- Our method of Mult. Int. Refl.:  $10^{-15}$  ;
- WKB-method (semiclassical, 1 order):  $10^{-3}$ .

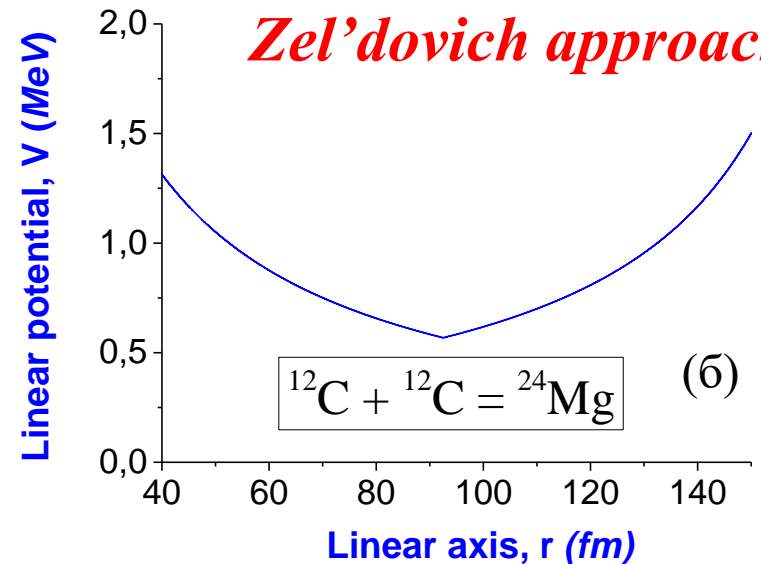


# Energy levels of zero-point vibrations (1)

*Our method:*



*Zel'dovich approach:*



*Determination of energy levels:*

Using method MR, energy levels are calculated, where modulus of WF is minimal or maximal at point  $R_0$ .

$$R_0 = 92.4 \text{ fm.}$$

$$E_0 = \frac{\hbar \omega}{2} = \frac{\hbar Z e}{\sqrt{m R_0^3}},$$

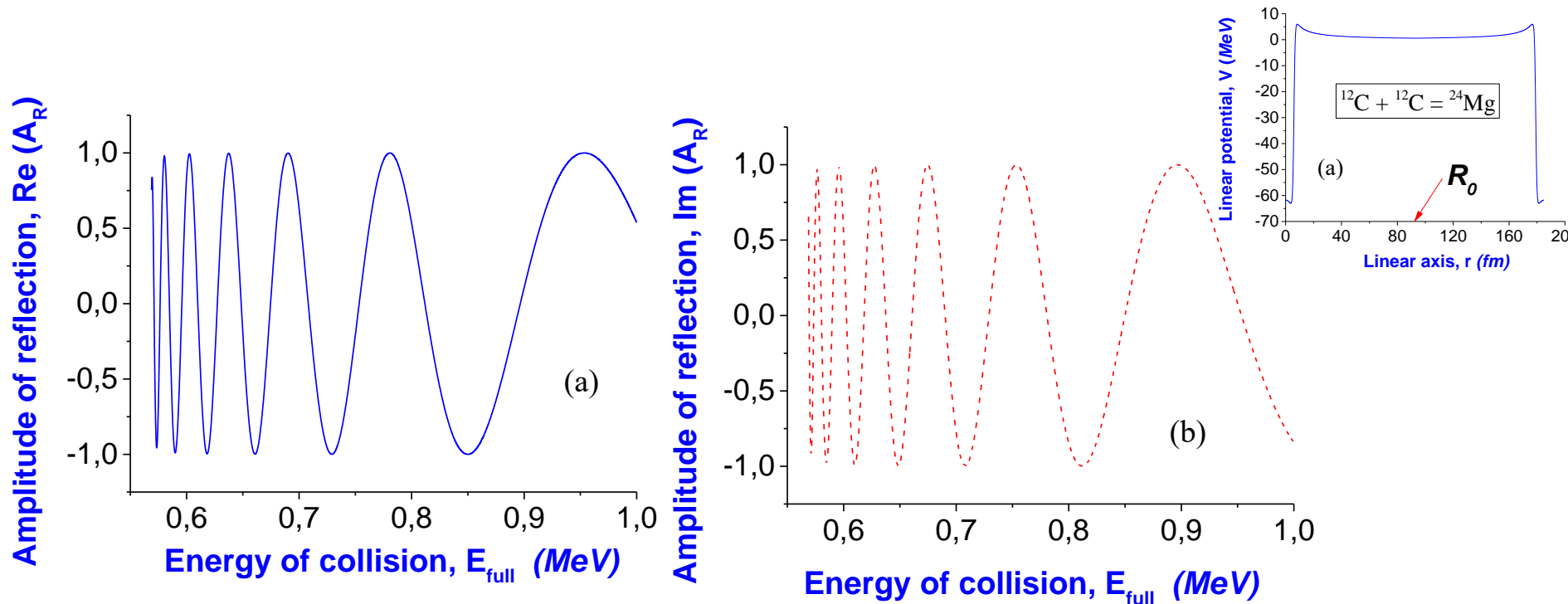
$$\Delta E = \frac{2Z^2 e^2}{R_0}, \quad E_{full} = E_0 + \Delta E.$$

$$E_0 = 0.021 \text{ MeV,}$$

$$\Delta E = 0.567 \text{ MeV,}$$

$$E_{full} = 0.589 \text{ MeV.}$$

# Energy levels of zero-point vibrations (2)



Condition for determination of states:

even states :  $\chi(R_0) = e^{-ikR_0} + A_R e^{ikR_0} = e^{-ikR_0} + e^{ikR_0}$ ,  $A_R = +1$ ,

odd states :  $\chi(R_0) = e^{-ikR_0} + A_R e^{ikR_0} = e^{-ikR_0} - e^{ikR_0}$ ,  $A_R = -1$ .

$\text{Re}(A_R) = \pm 1$ ,  
 $\text{Im}(A_R) = 0$ .

**Idea of determination of levels:** Using method MR, energy levels are determined, where condition of amplitude  $A_R$  at point  $R_0$  is fulfilled.

# Energy levels of zero-point vibrations (3)

No.	Energy, MeV	Amplitude AR, Re	Amplitude AR, Im
1	0.569699398797595	0.933197319275621	-0.359364387908423
2	0.574108216432866	-0.929937621506901	0.367717310044127
3	0.580280561122244	0.999976682784241	-0.006828900923611
4	0.589979959919840	-0.999804559327251	0.019769753373290
5	0.603206412825651	0.987566383351778	-0.155269148780593
6	0.619078156312625	-0.987872204000573	0.065877586140615
7	0.637595190380762	0.999675512392435	-0.025472925291808
8	0.661402805611222	-0.997827712405446	0.030972157654334
9	0.690501002004008	0.999520247643956	0.012515115484128
10	0.729298597194389	-0.999921682875423	-0.037392568402883
11	0.781322645290581	0.999300653371264	0.006701609064401
12	0.850100200400802	-0.999977543965837	-0.016661252673514
13	0.954148296593186	0.999861191695802	

$E_0^{(Zel'dovich)} = 0.589 \text{ MeV}$ .

Error in calculation of amplitudes:  $\left| |A_T|^2 + |A_R|^2 - 1 \right| < 10^{-14}$ .

# Conclusions

---

- 1) Rates of pycnonuclear reactions are changed essentially after taking into account nuclear forces (i.e., nuclear potential between nuclei).
- 2) Quantum study reduces rates of reactions up to 1,8 times. This is explained so: the most probable fusion of the nuclei does not happen after leaving nuclear fragment from the tunnel region, but after further propagation to the middle of the internal potential well.
- 3) Quantum study of the pycnonuclear reaction requires complete analysis of quantum fluxes in the internal region in the nuclear system. This leads to the appearance of new *quasibound states*, there formation of compound nuclear system is the most probable.
- 4) Reaction in quasibound states is essentially more probable, than at energies of zero-point vibrations studied by Zel'dovich and followers. There is a sense to tell about reaction rates for quasi-bound states, rather than for states of zero-point vibrations in lattice sites. This leads to the changes in estimation of the rates of pycnonuclear reactions in stars.
- 5) Energy spectrum of zero-point vibrations is revised.

---

Thank you for  
attention!